

Formation of methyl formate after cosmic ion irradiation of icy grain mantles

P. Modica and M. E. Palumbo

INAF – Osservatorio Astrofisico di Catania, via Santa Sofia 78, 95123 Catania, Italy
e-mail: mepalumbo@oact.inaf.it

Received 19 January 2010 / Accepted 25 May 2010

ABSTRACT

Context. Methyl formate (HCOOCH_3) is a complex organic molecule detected in hot cores and hot corinos. Gas-phase chemistry fails to reproduce its observed abundance, which usually varies between 10^{-7} and 10^{-9} with respect to H_2 .

Aims. Laboratory experiments were performed in order to investigate a solid-state route of methyl formate formation, to obtain an estimate of the amount that can be formed, and to verify whether it can account for the observed abundances.

Methods. Several solid samples (16 K) of astrophysical interest were analyzed by infrared spectroscopy in the $4400\text{--}400\text{ cm}^{-1}$ range. The infrared spectral characteristics of frozen methyl formate were studied by deriving their band strength values. The effects produced upon warm-up of the samples were analyzed comparing the spectra taken at different temperatures. In order to study the formation and destruction mechanism of methyl formate in the interstellar ices, a binary mixture of methanol (CH_3OH) and carbon monoxide (CO) ice and a sample of pure methanol were irradiated at 16 K with 200 keV protons. Methyl formate was identified through its fundamental mode (CH_3 rocking) at about 1160 cm^{-1} .

Results. We present the mid-infrared methyl formate ice spectrum showing both the amorphous (16 K) and the crystalline (110 K) structure. We report novel measurements of the band strength values of the six main methyl formate bands. We prove the formation and the destruction of methyl formate after irradiation of CH_3OH and a $\text{CO}:\text{CH}_3\text{OH}$ mixture. Extrapolating our results to the interstellar medium conditions we found that the production timescale of methyl formate agrees well with the evolutionary time of molecular clouds. The comparison with the observational data indicates that the amount of methyl formate formed after irradiation can account for the observed abundances.

Conclusions. The present results allow us to suggest that gas phase methyl formate observed in dense molecular clouds is formed in the solid state after cosmic ion irradiation of icy grain mantles containing CO and CH_3OH and released to the gas phase after desorption of icy mantles.

Key words. astrochemistry – molecular data – ISM: abundances – ISM: clouds – methods: laboratory

1. Introduction

Dust grains inside dense molecular clouds are covered by icy mantles. These are volatile structures consisting of simple molecules and atoms such as carbon monoxide, oxygen, and nitrogen. Other molecules can be produced on the grain surface by successive hydrogenation of condensed species and/or interaction with low-energy cosmic rays and UV photons (e.g. Tielens & Hagen 1982; Grim & Greenberg 1987; Palumbo & Strazzulla 1993). The radiation field modifies the pristine ices ionizing the molecules and producing radicals that after recombination can form new species. As a consequence icy mantles are composed of water, carbon monoxide, carbon dioxide, traces of formaldehyde, methanol, ammonia, and possibly even more complex molecules (e.g. Boogert et al. 2008; Gerakines et al. 1999). When a young stellar object begins to form, the dust reaches the appropriate sublimation temperature of the ices, then the icy mantles sublime releasing their components into the gas phase. They may condense onto the grain surface again during the proto-planetary disk phase. Perhaps they are incorporated into the planetesimal forming the building blocks of planets, or into comets and asteroids.

In the astrophysical context, organic molecules with more than four atoms are usually considered complex and are called complex organic molecules (COMs). Some COMs are

interesting to biology because they are linked to the origin of life. They are known to exist in hot cores of star-forming regions (e.g. Ikeda et al. 2001), which are characterized by relatively high temperature ($T \geq 100\text{ K}$) and density ($n \geq 10^6\text{ cm}^{-3}$). In these objects icy mantles have sublimated. For over two decades, COMs have been detected only in massive hot cores, while recently they have also been observed in three hot corinos, low-mass star-forming regions (Cazaux et al. 2003; Kuan et al. 2004; Bottinelli et al. 2004a,b). Because hot corinos have sizes of a few tens of AU, the size of the solar nebula, it is particularly relevant to study the COMs formation and destruction mechanism because of the link to the formation of the Solar System. Such complex molecules would provide early proto-planetary nebulae with a rich organic inventory similarly to that expected to have occurred in our presolar nebula. Clues that connect the interstellar chemistry to the Solar System can be found in the cometary detection of COMs (Sandford et al. 2006) because comets are believed to contain the most pristine material remaining from the presolar nebula. They may have carried prebiotic organic chemistry from the interstellar clouds to the early Earth.

Of the COMs detected so far, special attention has been paid to the formation of the $\text{C}_2\text{H}_4\text{O}_2$ isomers – methyl formate (HCOOCH_3), acetic acid (CH_3COOH), and glycolaldehyde (HOCH_2CHO) – molecules that have the same chemical formula but differ in the way atoms are connected. These molecules

may provide important clues to the formation chemistry of large biomolecules. From recent observations in Sgr B2 N(NLH), it is estimated that the relative abundances of the three molecules are 1864:103:1 (methyl formate: acetic acid: glycolaldehyde) and the fractional abundances relative to H_2 are 3.7×10^{-8} , 2.0×10^{-9} , 2.0×10^{-11} for methyl formate, acetic acid, and glycolaldehyde respectively (Bennett & Kaiser 2007).

This paper focuses on methyl formate ($HCOOCH_3$), the most abundant of $C_2H_4O_2$ isomers in hot cores. Methyl formate may provide a connection to acetic acid (CH_3COOH) and even to glycine (NH_2CH_2COOH), the simplest biologically important amino acid. The first detection of interstellar methyl formate was made by Brown et al. (1975) toward the star-forming region Sgr B2. After it has been detected in several hot cores, in three hot corinos (Bottinelli et al. 2007), and in comets (Bockelée-Morvan et al. 2000; Despois et al. 2005; Remijan et al. 2006). All these detections suggest that methyl formate may be widely distributed in the Galaxy.

One of the open questions about methyl formate is to explain its abundance in the interstellar medium. Although it is generally accepted that methyl formate can be produced from methanol formed in the icy grain mantles, models based only on gas-phase reactions are unable to account for the observed abundances. Until a few years ago it was thought that methyl formate could be formed in the gas phase after the sublimation of icy mantles containing H_2CO and CH_3OH . Horn and colleagues studied the specific sequence of reactions that was supposed to lead to the synthesis of methyl formate (Horn et al. 2004). The results of their theoretical and experimental gas-phase study have conclusively shown that the processes in the gas phase are unable to produce sufficient amounts of methyl formate. This evidence has profoundly changed the standard production scenario suggesting that methyl formate should be produced mainly by reactions in ices rather than in gas phase. Nowadays new routes of formation and destruction have been proposed in literature, pointing to a much more important role for grain surface reactions and energetic processing of icy mantles than previously believed. Mixtures of methanol and carbon monoxide ices were irradiated at 10 K with energetic electrons (Bennett & Kaiser 2007), establishing the formation of glycolaldehyde and methyl formate. Furthermore methyl formate has been observed after UV photolysis of pure CH_3OH and $CO:CH_3OH$ ice mixtures (Gerakines et al. 1996; Öberg et al. 2009).

Methyl formate has not yet been observed in the solid state as a component of icy grain mantles because its strongest bands overlap with those from other present and more abundant molecules. Both CO and CH_3OH are found to be abundant within the grain mantles. Recently, it was experimentally shown that CH_3OH can be produced efficiently by successive hydrogenation of CO (Watanabe et al. 2007; Fuchs et al. 2009). As a consequence, these two components are supposed to reside well mixed in the icy mantles.

In this work we will investigate the formation and destruction of methyl formate in the solid state after cosmic ion irradiation of icy grain mantles containing CO and CH_3OH . Our purpose is to study in the laboratory the formation mechanism suggested, to quantitatively evaluate the amount of methyl formate that can be formed, and to assess whether it is able to produce methyl formate in such quantities to justify the observed abundances in the interstellar medium. In this regard we conducted experiments that simulate the chemical-physical effects induced on icy mantles after cosmic ion irradiation. In order to study the formation of methyl formate within interstellar ices, we chose to investigate the effects of 200 keV protons

on a binary ice mixture of carbon monoxide and methanol ($CO:CH_3OH = 1.6:1$) and a sample of pure methanol at 16 K. These effects were studied by infrared spectroscopy. We have performed new laboratory experiments, which enabled us to obtain an estimate of the amount of methyl formate formed after irradiation.

2. Experimental procedure

2.1. Experimental set-up

The present experiments were performed in the Laboratory for Experimental Astrophysics at INAF-Osservatorio Astrofisico di Catania (Italy). The experimental apparatus used to obtain infrared transmission spectra is composed of a stainless steel high-vacuum chamber operating at a pressure $P < 10^{-7}$ mbar interfaced with a FTIR spectrometer ($4400-400\text{ cm}^{-1} = 2.27-25\text{ }\mu\text{m}$) through IR-transparent windows. The gas or gas mixture to be investigated is injected into the chamber through a needle valve and subsequently frozen onto a chosen substrate (Si or KBr) that is in thermal contact with a cold finger (10–300 K).

After deposition the samples were bombarded by 200 keV H^+ ions. The ions are obtained from an ion implanter interfaced with the vacuum chamber. The beam used produces current densities in the range from 10^{-1} to a few $\mu\text{A cm}^{-2}$ in order to avoid macroscopic heating of the target. The ion beam and the infrared beam are mutually perpendicular while they form an angle of 45 degrees with the substrate plane. In this way, spectra can be taken at any time, before, during, and after irradiation, without tilting the sample. The energy released to the sample by impinging ions (dose) is given in eV/16 u, where u is the unified atomic mass unit defined as 1/12 of the mass of an isolated atom of carbon-12. As discussed by Strazzulla & Johnson (1991), the dose given in units of eV per small molecule (16 u) is a convenient way to characterize chemical changes and compare the results obtained irradiating different samples.

For each sample, after each step of irradiation, two spectra are taken, one with the electric vector parallel (P polarized) and one perpendicular (S polarized) to the plane of incidence, where the polarization of the infrared radiation is selected by rotating a polarizer placed in the path of the infrared beam in front of the detector. All spectra in this work are ratioed to the corresponding spectrum of the background acquired before deposition and were taken at a resolution of 1 cm^{-1} . Each spectrum is plotted on an optical depth scale using the relation $I = I_0 \cdot e^{-\tau}$ (Beer-Lambert law), where $\tau = \alpha \cdot x$ (α = absorption coefficient; x = path length through the material).

A detailed description of the experimental apparatus used can be found elsewhere (Strazzulla et al. 2001; Palumbo et al. 2004).

2.2. Thickness measurement

In this experimental set-up it is possible to measure the thickness of the frozen samples. Here we followed the same procedure described in Fulvio et al. (2009). During deposition a He-Ne laser beam ($\lambda = 543\text{ nm}$) is directed towards the sample and reflected by the vacuum-sample and the sample-substrate interfaces (Fig. 1). After the reflection the laser beam is detected by an external silicon-diode detector. Between the reflected components of the laser beam there is a difference of optical path, which grows with increasing thickness. Because of this, interference is produced. By looking in real time at the interference

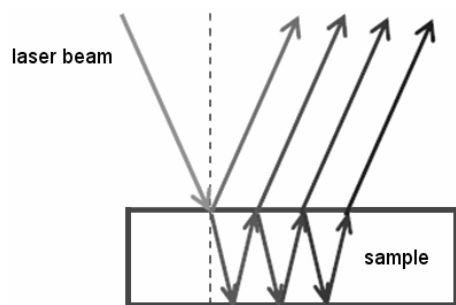


Fig. 1. Scheme of the multiple reflections of the laser beam by the vacuum-sample and the sample-substrate interfaces.

curve (intensity versus time) it is possible to monitor the accretion of the sample during deposition. We used two different substrates for deposition: Si and KBr.

To measure the thickness of the sample it is first of all necessary to determine its refractive index n_f . We can obtain this value from the interference curve with a numerical method (Baratta & Palumbo 1998). Because the amplitude of the experimental interference curve depends on the refractive index n_f and on other known quantities (the refractive index n_s of the substrate, the incidence angle θ_i , and the polarization of the laser light), n_f can be derived measuring the intensity ratio between maxima and minima in the experimental interference curve. For HCOOCH_3 deposited on Si at 16 K, the value found is $n_f = 1.30$.

Once n_f was derived, we could also obtain the theoretical interference curve (reflectance) versus thickness. For non-absorbing materials this curve is a periodic function. We could measure the thickness of the deposited sample by comparing the theoretical interference curve with the experimental one, normalized from 0 to 1. For each chosen point on the experimental interference curve, we normalized the intensity value of radiation from 0 to 1. Then in the theoretical curve we identified the point at which this ordinate corresponds. The abscissa of the point found is the value of the thickness. We considered five thickness values.

The absolute accuracy of the thickness measured in this way is about 5%. It is limited mainly by the uncertainties in the knowledge of the optical constants of the substrate at low temperature and by the error in measuring the incidence angle of the laser beam. The thickness is corrected by a factor of

$$\frac{1}{\cos \theta_t} = \frac{1}{\sqrt{1 - \frac{\sin^2 \theta_i}{n_f^2}}}, \quad (1)$$

where θ_t is the refractive angle. This correction takes into account the increased path length of the IR beam at an incidence angle $\theta_i = 45$ deg.

3. Results

3.1. HCOOCH_3

Methyl formate (HCOOCH_3) is the methyl ester of formic acid (HCOOH). Its mid-infrared spectrum at 16 K (see Fig. 2) shows six main absorption bands due to molecular vibrations. The strong band at 1720 cm^{-1} is due to the C=O stretching vibration (ν_4 mode). The two strong bands at 1210 and 1164 cm^{-1} are due to the C–O stretching vibration (ν_8 mode) and the CH_3 rocking vibration (ν_9 mode) respectively. The double peak at 1435 and 1450 cm^{-1} is due to the CH_3 deformation (ν_{14}, ν_6 modes).

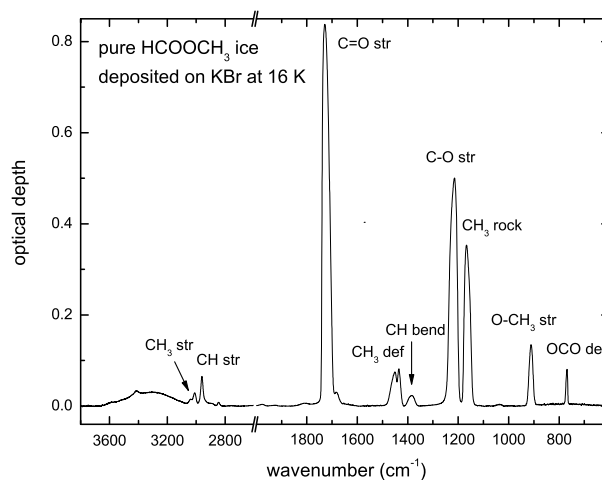


Fig. 2. IR spectrum of a pure HCOOCH_3 ice deposited at 16 K from 3800 to 600 cm^{-1} (2.6 – $16.7 \mu\text{m}$).

Table 1. Band positions of solid methyl formate deposited at 16 K and their assignments.

Band position cm^{-1}	μm	Assignment	Characterization
3038	3.29	ν_1	CH_3 str
3010	3.32	ν_2, ν_{13}	CH_3 str
2960	3.38	ν_3	CH str
1720	5.81	ν_4	C=O str
1450	6.90	ν_6	CH_3 def
1435	6.97	ν_{14}	CH_3 def
1383	7.23	ν_7	CH bend
1210	8.26	ν_8	C–O str
1164	8.59	ν_9	CH_3 rock
910	10.99	ν_{10}	O– CH_3 str
768	13.02	ν_{11}	OCO def

The two sharp bands at 910 cm^{-1} and 768 cm^{-1} are due to the O– CH_3 (ν_{10} mode) and the OCO deformation (ν_{11} mode) respectively. Table 1 reports the main methyl formate features.

3.2. Band strengths

From the derived n_f value, we can also estimate the sample density with the Lorentz-Lorenz relation

$$L\rho = \frac{n_f^2 - 1}{n_f^2 + 2}. \quad (2)$$

For a given species the Lorentz-Lorenz coefficient L is nearly constant for a fixed wavelength regardless of the material phase and temperature. Furthermore, although L is a function of wavelength, we can assume to a first approximation that it does not vary between 543 nm and 590 nm for a material transparent in the visible. With the refractive index and the density values for HCOOCH_3 at 590 nm and room temperature, available from commercial catalogs, we obtain $L = 0.217 \text{ cm}^3 \text{ g}^{-1}$. By substituting this L value in Eq. (2) and the value of the refractive index measured, we obtain for our experimental deposition conditions the density $\rho = 0.87 \text{ g cm}^{-3}$ for frozen HCOOCH_3 at 16 K.

With the values of thickness d (cm) and density ρ (g cm^{-3}) calculated above, we can derive the column density N

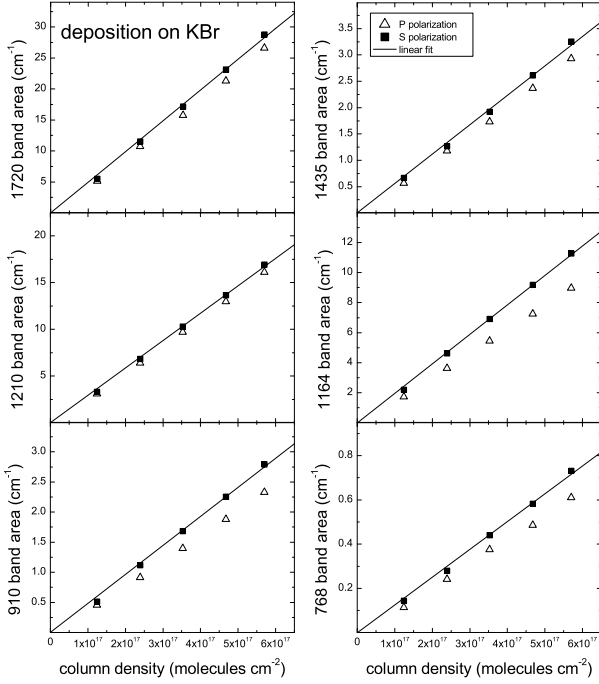


Fig. 3. Individual measures of the band area versus the column density for the HCOOCH₃ main bands from spectra taken in P and in S polarization. Superimposed is the line through the origin that best fits the points in S polarization.

(molecules cm⁻²) for a species of molecular weight μ (g) with the relation

$$N = \frac{d\rho}{\mu} . \quad (3)$$

The integrated intensity (area) measured of each selected band (in optical depth $\tau(\nu)$ scale) for a not-saturated band is proportional to the column density, and the following relation is valid:

$$\int \tau(\nu) d\nu = A \times N. \quad (4)$$

Measuring the integrated intensity of each selected band from the infrared spectra for different thickness values, we get the integrated band strength A (cm molecule⁻¹) value:

$$A = \frac{\int \tau(\nu) d\nu}{N} . \quad (5)$$

To derive the band strength values for the main infrared features of frozen HCOOCH₃ at 16 K we plotted each band area against the column density (Figs. 3 and 4). Calculating the best fit of data, the angular coefficients of the straight lines obtained represent the band strength for each selected feature for the two different substrates used for deposition. The band strength values are reported in Table 2. For the double peak at 1435 and 1450 cm⁻¹ we have estimated the A value considering it as a single feature peaked at 1435 cm⁻¹. We note differences due to the substrate in the obtained A value between 6–25%. These differences can be explained by the limits of applicability of the Beer-Lambert law.

3.3. Warm-up effects

Because of its high gas phase abundance, the sublimation properties of HCOOCH₃ are important.

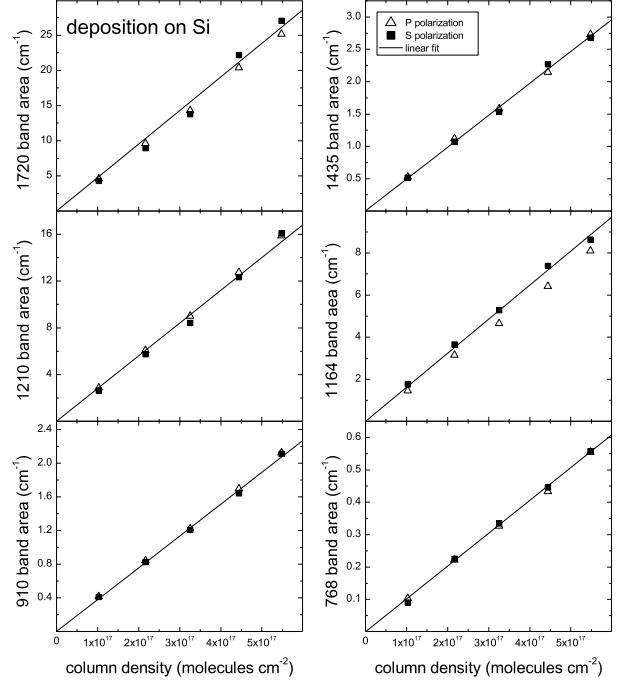


Fig. 4. Individual measures of the band area versus the column density for the HCOOCH₃ main bands from spectra taken in P and in S polarization. Superimposed is the line through the origin that best fits the points in S polarization.

Table 2. Band strength values (A) for the most intense features of frozen methyl formate deposited at 16 K on two different substrates (Si and KBr).

Band position (cm ⁻¹)	A (cm molecule ⁻¹)	
Substrate	Si	KBr
1720	4.77×10^{-17}	4.96×10^{-17}
1435	4.94×10^{-18}	5.58×10^{-18}
1164	1.62×10^{-17}	1.96×10^{-17}
1210	2.80×10^{-17}	2.93×10^{-17}
910	3.79×10^{-18}	4.82×10^{-18}
768	1.01×10^{-18}	1.25×10^{-18}

Methyl formate deposited at 16 K presents an amorphous structure. The sample was warmed-up and spectra were acquired at 30, 50, 70, 90, 110, and 155 K (in P and in S polarization). In Fig. 5 we compare two spectra taken before (16 K) and after (110 K) the warm-up. The individual panels show the profile of the most intense bands. The deep changes in the bottom panels are caused by the crystallization of the sample. It occurs within the temperature range between 90 and 100 K. At 130 K the sample sublimates.

3.4. CH₃OH:HCOOCH₃

A CH₃OH:HCOOCH₃ = 10:1 ice mixture was deposited on KBr at 16 K. The profile of methyl formate bands in mixture with methanol is slightly different from that of the pure sample, in particular the width of the bands decreases. Figure 6 shows the spectral region from 1170 to 1000 cm⁻¹ where we can make a comparison between the 1164 cm⁻¹ band, normalized to the maximum value, in the spectrum of the CH₃OH:HCOOCH₃ ice mixture and in the spectrum of the pure HCOOCH₃ ice. The full width at half maximum (FWHM) in the pure sample is 27 cm⁻¹,

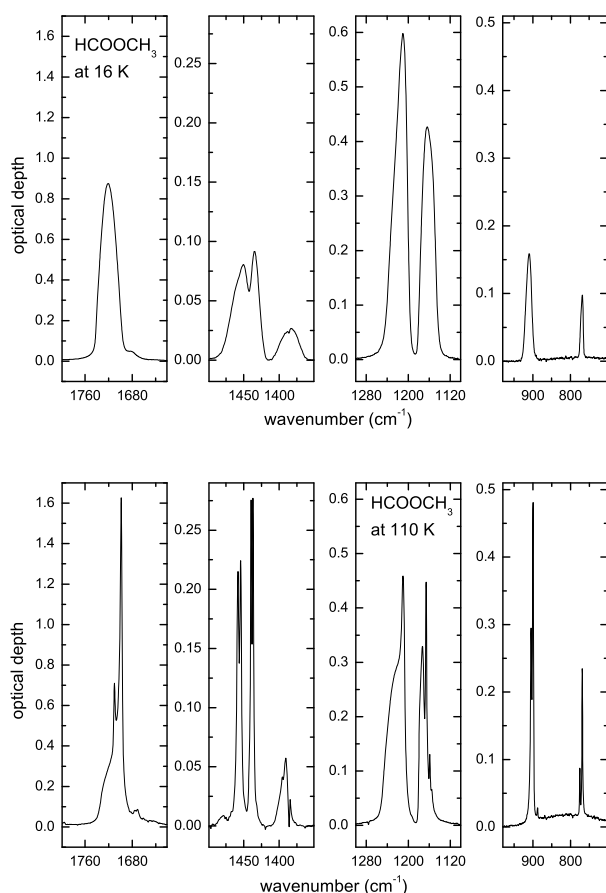


Fig. 5. Profiles of the most intense bands (in S polarization) in amorphous HCOOCH_3 (top panels) and in crystalline HCOOCH_3 (bottom panels). The y-scale in the panels is different for clarity.

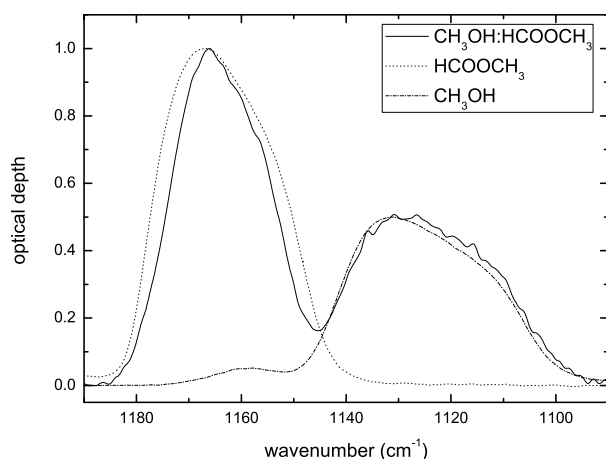


Fig. 6. Comparison between the profile of the band at 1164 cm^{-1} in pure HCOOCH_3 (dotted line) and in a $\text{CH}_3\text{OH}:\text{HCOOCH}_3 = 10:1$ mixture (solid line) at $T = 16\text{ K}$. The spectrum of CH_3OH (dashed dotted line) is shown for completeness. The optical depth is expressed in arbitrary units.

while in the mixture it is 21 cm^{-1} . For completeness the spectrum of methanol is also shown.

After deposition the ice mixture was warmed-up and spectra were taken at 80, 100, 120, and 140 K. In this experiment we found that methyl formate in a mixture with methanol sublimates between 120 and 140 K. This temperature is similar to that of the pure species.

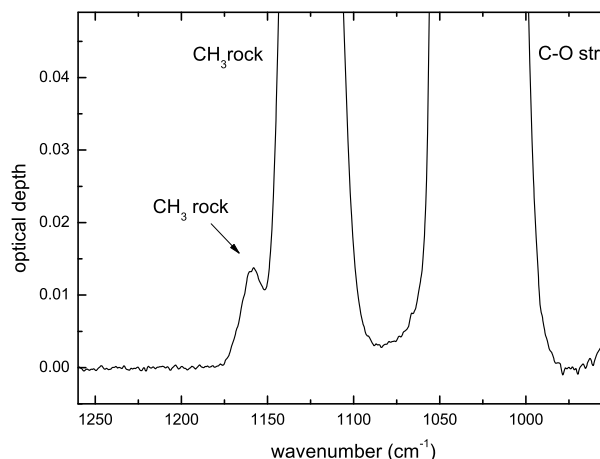


Fig. 7. Enlargement of the methanol spectrum in the $1250\text{--}950\text{ cm}^{-1}$ ($8.0\text{--}10.5\text{ }\mu\text{m}$) spectral region.

3.5. Ion irradiation effects

We irradiated pure CH_3OH and a $\text{CO}:\text{CH}_3\text{OH}$ mixture at 16 K with 200 keV H^+ ions.

The mid-IR spectrum of solid methanol (Sandford & Allamandola 1993; Palumbo et al. 1999; Bennett et al. 2007) presents a wide and intense band centered at 3269 cm^{-1} due to the OH stretching (ν_1 mode), two less intense bands due to the CH_3 stretching mode at 2959 cm^{-1} (ν_2, ν_9 modes) and 2830 cm^{-1} (ν_3 mode). In the region between 2600 and 2000 cm^{-1} there are weak bands due to combination modes and a band at 2049 cm^{-1} due to overtones. In the last portion of the spectrum there is a band at 1452 cm^{-1} due to the CH_3 deformation (ν_4, ν_5, ν_{10} modes), which presents a small shoulder at 1424 cm^{-1} due to the OH bending (ν_6 mode). There is a weak band at 1129 cm^{-1} due to the CH_3 rocking (ν_7, ν_{11} modes) and an intense band at 1033 cm^{-1} due to the CO stretching (ν_8 mode). Figure 7 is an enlargement of the $1250\text{--}950\text{ cm}^{-1}$ spectral region, where a weak band due to the CH_3 rocking vibration at about 1160 cm^{-1} is evident.

We compared the IR spectrum of pure methanol frozen at 16 K with that obtained after irradiation with 200 keV H^+ ions at a dose of $32.4\text{ eV}/16\text{ u}$. Because of ion irradiation, methanol molecules are broken and other species are formed as a consequence of recombination of produced radicals and molecular fragments. New bands appear in the spectrum taken after irradiation. The spectral region of interest was divided into three parts for clarity (Fig. 8). In panel (a) a band due to CH_4 appears at 3010 cm^{-1} (Palumbo et al. 1999). In panel (b) CO_2 bands appear at 2344 cm^{-1} ($^{12}\text{CO}_2$) and 2278 cm^{-1} ($^{13}\text{CO}_2$), while the CO band appears at 2136 cm^{-1} . In panel (c) we can observe the formation of H_2CO at 1720 cm^{-1} (Hudson & Moore 2000; Bennett & Kaiser 2007), CH_4 at 1304 cm^{-1} , and $\text{C}_2\text{H}_4(\text{OH})_2$ (ethylene glycol) at 1090 cm^{-1} (Hudson & Moore 2000). Moreover we can see a weak band near 1160 cm^{-1} that we attribute to HCOOCH_3 .

A $\text{CO}:\text{CH}_3\text{OH} = 1.6:1$ ice mixture was deposited at 16 K. At the end of deposition the thickness was $d = 1.65\text{ }\mu\text{m}$. The sample was irradiated with 200 keV H^+ ions and spectra were taken at increasing dose. Also here, new bands appear in the spectra taken after irradiation, which are listed in Table 3. The spectral region of interest was divided into four parts for clarity (Fig. 9). We compared the IR spectrum of the mixture ice at 16 K with that obtained after irradiation at $18.7\text{ eV}/16\text{ u}$. In panel (a) we

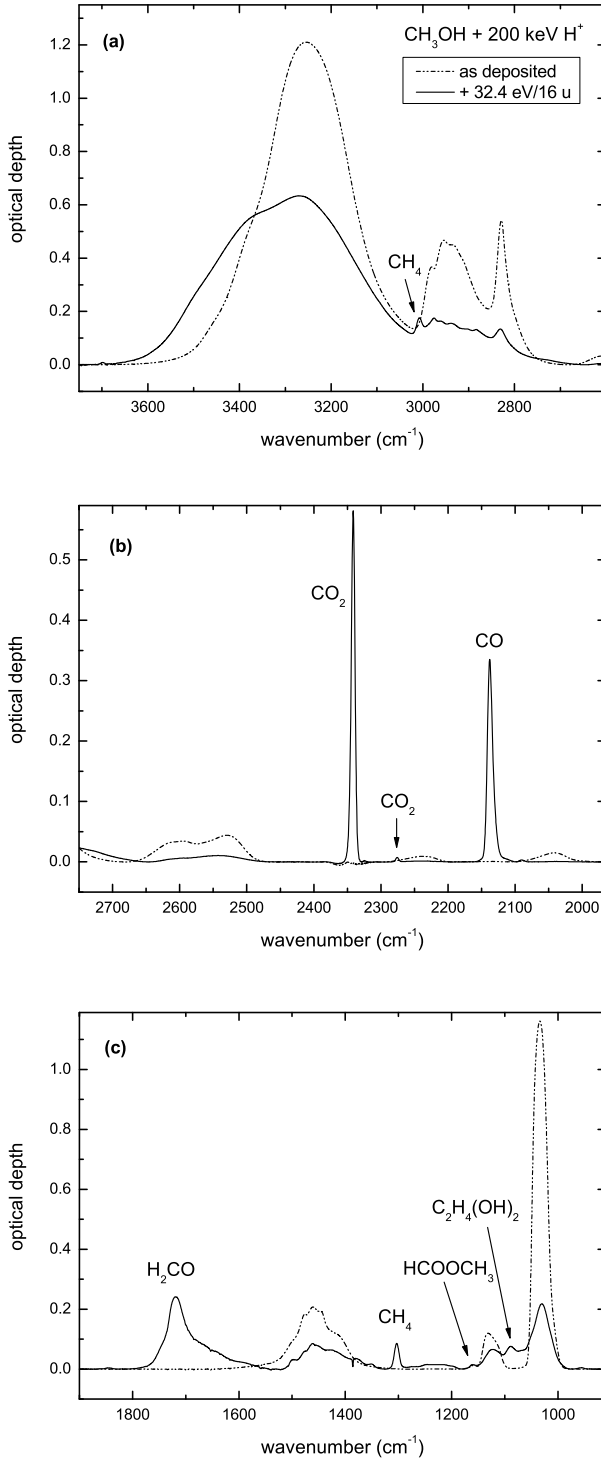


Fig. 8. Infrared spectra of a CH₃OH pure ice as deposited (dotted lines) and after irradiation with 200 keV protons (solid lines) in three different spectral regions from 3700 to 900 cm⁻¹ (2.70–11.11 μm).

see the new band centered at 3700 cm⁻¹ due to CO₂ and the band at 3010 cm⁻¹ due to CH₄. In panel (b) the bands of ¹²CO and ¹³CO₂ are out of scale. The new band at 2280 cm⁻¹ is due to ¹³CO₂, the band at 2089 cm⁻¹ is due to ¹³CO. In panel (c) there is the new band at 1843 cm⁻¹ due to HCO, the band at 1720 cm⁻¹ due to H₂CO, and the band at 1304 cm⁻¹ due to CH₄. In panel (d) there is the band at 660 cm⁻¹ due to CO₂ and the band at 1090 cm⁻¹ due to HCO. The inset in panel (d) shows the spectral region between 1180 and 980 cm⁻¹ after irradiation at

Table 3. Position, assignment and characterization of new bands observed after irradiation of CO:CH₃OH mixture at 16 K.

Band position cm ⁻¹	μm	Species	Assignment	Characterization
660	15.15	CO ₂	ν ₂	bend
1067	9.37	HCOCH ₂ OH	ν ₇	C–O str
1090	9.17	HCO	ν ₂	bend
1159	8.63	HCOOCH ₃	ν ₉	CH ₂ rock
1247	8.02	H ₂ CO	ν ₂	CH ₂ rock
1304	7.66	CH ₄	ν ₄	deform
1500	6.67	H ₂ CO	ν ₃	CH ₂ scis
1726	5.79	H ₂ CO	ν ₂	C=O str
1843	5.43	HCO	ν ₃	C=O str
2280	4.39	¹³ CO ₂	ν ₃	C=O str
2325	4.30	OC ¹⁸ O	ν ₃	C=O str
2342	4.27	CO ₂	ν ₃	C=O str
3010	3.32	CH ₄	ν ₃	C–H str
3700	2.70	CO ₂		combination

5.2 eV/16 u. In this region two weak bands due to C₂H₄O₂ isomers are visible: the band at 1067 cm⁻¹ due to glycolaldehyde (HCOCH₂OH) and the band at about 1160 cm⁻¹ that we attribute to methyl formate (HCOOCH₃). The position of this band is in accordance with a methyl formate band (see Fig. 2) due to the rocking of CH₃ (ν₉ fundamental mode).

In the spectra of the CO:CH₃OH mixture three methanol bands are present, at 2830 cm⁻¹ (CH₃ stretching), at 1128 cm⁻¹ (CH₃ rocking), at 1033 cm⁻¹ (C–O stretching), which are not superimposed to the bands of other species. We measured their band areas in the spectra after deposition and during irradiation. Figure 10 shows the data obtained as a function of dose after normalization to the initial value. The data show that after irradiation methanol is efficiently destroyed. The same trend is observed after irradiation of pure methanol.

3.6. 1160 cm⁻¹ band area

A band at about 1160 cm⁻¹ is present in the spectra of pure CH₃OH and CO:CH₃OH mixture after ion irradiation. This band is a key element that proves the formation of methyl formate in the solid phase after irradiation. We measured the area of the band in the spectra of the mixture and plotted the obtained values as a function of irradiation dose. Data are shown in Fig. 11 by the open squares. This band overlaps another weak band, the methanol fundamental mode ν₁₁ (visible in the enlargement in Fig. 7). Therefore the total area of the 1160 cm⁻¹ band (1160 a_T) receives the contribution by two molecular species: methanol (M), already present in the sample as deposited, and methyl formate (MF), formed after ion irradiation. Because we are interested in the study of the HCOOCH₃ band, we need to remove the contribution by methanol to the total band area before and after irradiation. Here we describe this procedure. The following relation is valid:

$$1160 a_T = 1160 a_M + 1160 a_{MF}. \quad (6)$$

The 1160 cm⁻¹ band area in the spectrum before irradiation receives only the contribution by methanol, so for the initial value (*i*) we have

$$1160 a_{Ti} = 1160 a_{Mi}. \quad (7)$$

The band at 1033 cm⁻¹ is an isolated methanol band that we can use as representative of the methanol behavior in the spectra

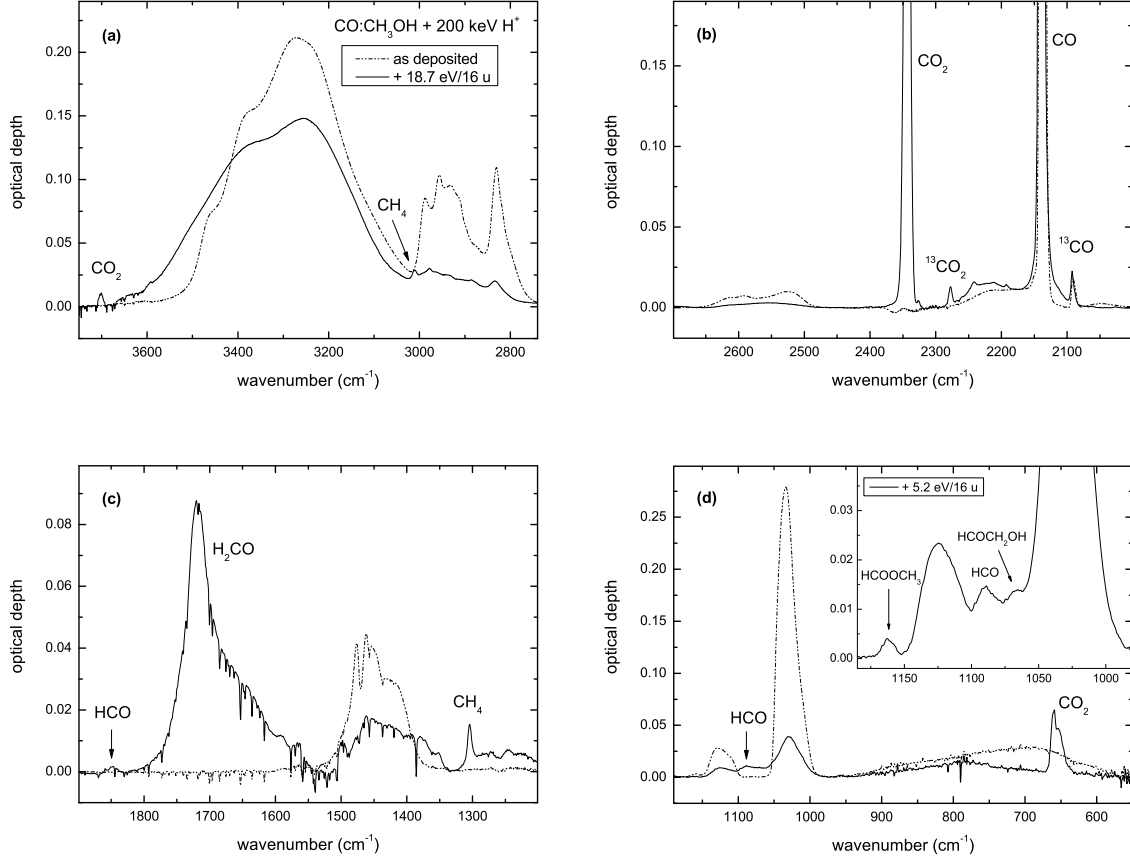


Fig. 9. Infrared spectra of the CO:CH₃OH ice before irradiation (dotted lines) and after irradiation with 200 keV protons (solid lines) in four different spectral regions from 3800 to 550 cm⁻¹ (2.63–18.18 μm). The inset of panel **d**) shows the spectral region 1180–980 cm⁻¹ after a dose of 5.2 eV/16 u.

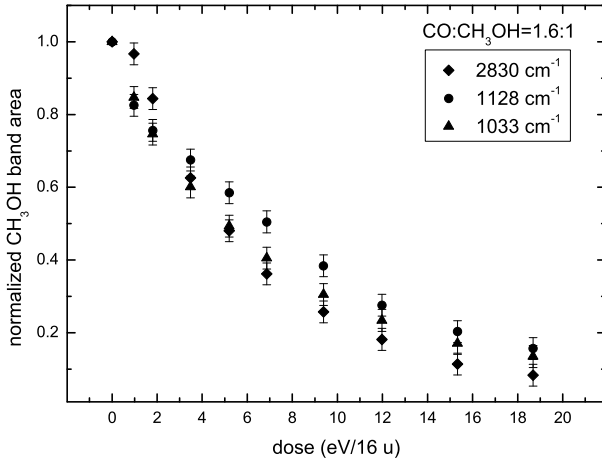


Fig. 10. Plot of the band area, normalized to the first value, versus dose for three methanol bands.

of the mixture (see Sect. 3.5 and Fig. 10). We calculated the ratio (R) between 1160 cm⁻¹ and 1033 cm⁻¹ band areas in the spectrum before irradiation:

$$\frac{1160 a_{Mi}}{1033 a_{Mi}} = R. \quad (8)$$

Before irradiation the value of R is 0.0016. Assuming that R is maintained constant also after irradiation, we can evaluate the

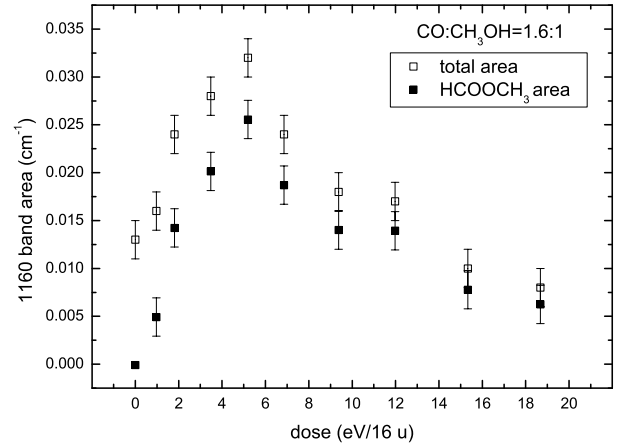


Fig. 11. 1160 cm⁻¹ band area versus dose. Open squares refer to the total area, filled squares refer to the area due to methyl formate.

contribution by methanol to the 1160 cm⁻¹ band area at different doses:

$$1160 a_M = R \times 1033 a_M. \quad (9)$$

By substituting this value in Eq. (6) we can easily subtract the contribution by methanol to the 1160 cm⁻¹ total band area in each spectrum. After the subtraction we obtained the area values due to methyl formate (filled squares in Fig. 11). The data show a two-step pattern: in the first step the trend is growing up, in the second step it is slowly descending. Because in optical depth

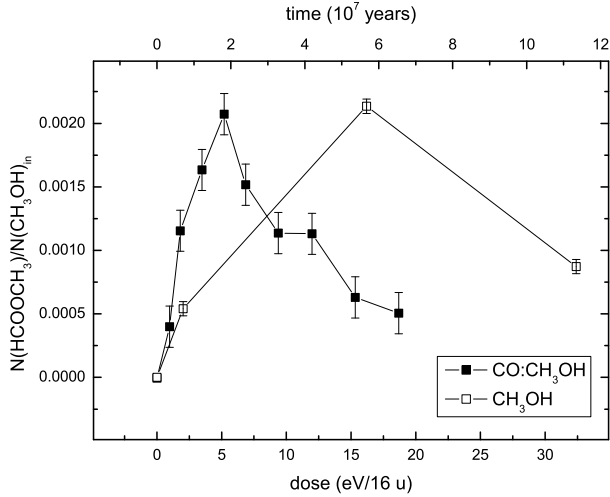


Fig. 12. Methyl formate column density ratioed to methanol initial column density versus time (top x -axis) and different suffered doses (bottom x -axis) in the mixture (filled squares) and in pure methanol (open squares). Solid lines have been drawn only to guide the eye.

scale the intensity of a not saturated band increases linearly with the amount of the responsible molecules present in the sample, we interpreted this trend as indicating the formation of methyl formate in the first step and its gradual destruction in the second step. Our previous experiments (see Sects. 2.2 and 3.2) enabled us to obtain an estimate of the amount of methyl formate present in the mixture after irradiation. The column density of methyl formate was easily monitored using the equation

$$N = \frac{\int \tau(\nu) d\nu}{A}, \quad (10)$$

where $A = 1.96 \times 10^{-17}$ cm molecule $^{-1}$ is the 1164 cm $^{-1}$ band strength value given in Table 2. We chose to express the abundance of methyl formate with respect to methanol initial abundance. The column density of methanol has been estimated from the 1033 cm $^{-1}$ band using $A = 1.3 \times 10^{-17}$ cm molecule $^{-1}$ (Palumbo et al. 1999). Figure 12 shows the estimated $N(\text{HCOOCH}_3)/N(\text{CH}_3\text{OH})$ ratio relative to initial methanol as a function of the dose. We show a comparison between the mixture and the pure methanol samples. For the mixture, the ratio reaches the order of 10^{-3} at low doses (about 2 eV/16 u).

4. Discussion

We performed several laboratory experiments. In particular we analyzed a sample of frozen pure methanol (CH_3OH) and a mixture of methanol and carbon monoxide ($\text{CO}:\text{CH}_3\text{OH} = 1.6:1$). Maintaining a constant temperature (16 K), both samples were irradiated with 200 keV protons and analyzed by infrared spectroscopy before, during, and after irradiation. The results of the experiments showed that in both samples the irradiation can induce the formation of methyl formate, which has been identified through the band at about 1160 cm $^{-1}$.

In Fig. 13 we overlaid the spectrum of the mixture after a dose of 5.2 eV/16 u and the spectrum of methyl formate as deposited, zooming in for clarity the region between 1800 and 950 cm $^{-1}$ where the three most intense bands of methyl formate are. We did not show the spectral region beyond 950 cm $^{-1}$ because unfortunately the spectra are too noisy, so it is not possible to quantitatively analyze the bands at 910 cm $^{-1}$ and at 768 cm $^{-1}$

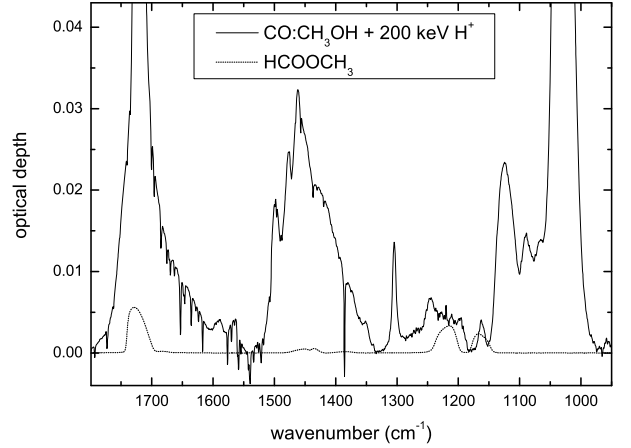


Fig. 13. Contribution of methyl formate to the intensity of the bands in the irradiated $\text{CO}:\text{CH}_3\text{OH}$ mixture.

of methyl formate. Considering that methyl formate contributes with about 80% to the 1160 cm $^{-1}$ band area in the spectrum, we appropriately reduced the y -scale of the HCOOCH_3 spectrum until this condition was realized and until its other bands fell within the corresponding bands in the spectrum of the mixture. As we can see, the spectrum of methyl formate is compatible with the spectrum of the irradiated mixture, indeed the three bands of HCOOCH_3 are perfectly centered at the position of the bands present in the spectrum of the irradiated mixture. The band at 1160 cm $^{-1}$ in the spectrum of HCOOCH_3 presents a FWHM greater than that in the spectrum of the irradiated $\text{CO}:\text{CH}_3\text{OH}$ mixture. As discussed in Sect. 3.4 for the $\text{CH}_3\text{OH}:\text{HCOOCH}_3$ mixture, this evidence can be considered as a natural behavior of the band when methyl formate is mixed with other species.

Despite the non-rigorous method used, but in agreement with our previous results, we managed to find the hypothetical contribution to the band intensity of the irradiated mixture due to methyl formate. Unfortunately we could not find bands solely attributable to methyl formate because the abundance of the molecules in the sample is small and the strongest bands of the molecule are shared with those of other species. In particular, the broad feature around 1230 cm $^{-1}$ present after irradiation of the mixture could be due to the contribution by H_2CO (formaldehyde), HCOOH (formic acid), CH_3COCH_3 (acetone), and CH_2OH (methoxy radical) (Öberg et al. 2009; Bennett et al. 2007; Hudson & Moore 2000; Palumbo et al. 1999; Gerakines et al. 1996).

As shown in Fig. 12, for both samples the amount of methyl formate, which is progressively produced by irradiation, is on the order of 10^{-3} with respect to the amount of methanol initially present in the samples as deposited. These results, applied to the astrophysical analysis, suggest that during continuous exposure of the icy mantles to low-energy cosmic rays, one part out of 10^3 of initial methanol could be converted into methyl formate, while the part that does not participate in the formation of this molecule should be gradually destroyed, forming other molecular species, the most abundant of which are CO , CO_2 , CH_4 , H_2CO (Palumbo et al. 1999; Hudson & Moore 2000; Baratta et al. 2002).

In order to estimate the time necessary to obtain the effects observed in the laboratory in dense molecular clouds we consider the approximation of effective monoenergetic 1 MeV protons and assume that in dense interstellar regions

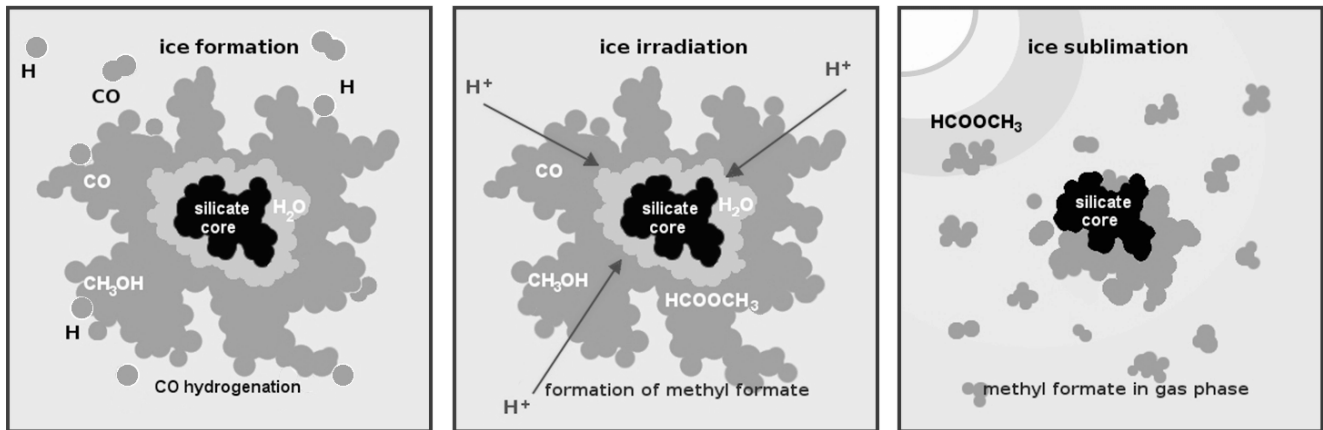


Fig. 14. Formation of methyl formate on icy grain mantles and release to the gas-phase. *Left panel:* CO hydrogenation and formation of CH₃OH. *Middle panel:* interaction with cosmic rays and formation of HCOOCH₃. *Right panel:* rise of temperature and HCOOCH₃ sublimation.

the 1 MeV flux is equal to 1 proton $\text{cm}^{-2} \text{s}^{-1}$ (Mennella et al. 2003). Our experimental results were obtained using 200 keV protons. Thus in order to extrapolate the laboratory results to the interstellar medium conditions we assume that they scale with the stopping power (S , energy loss per unit path length) of impinging ions. With these hypotheses we indicated in Fig. 12 the timescale axis (top x -axis), which gives an estimation of the time (10^7 years) necessary to obtain the effects observed in the laboratory on interstellar ices. We obtained that about 2×10^7 years would be necessary to form the observed column density of methyl formate. This time agrees with the evolutionary timescale (3×10^7 – 5×10^8 years) of molecular clouds (Greenberg 1982). Methyl formate has also been observed in Class 0 objects (e.g. Bottinelli et al. 2004a,b, 2007). It has been estimated that these objects have a dynamical age of a few thousand years (e.g. Maret et al. 2002; Bottinelli et al. 2004a,b). According to current models, low-mass stars form inside molecular clouds from dense and cold condensations, called prestellar cores, which evolve into Class 0 and then Class I sources. Prestellar cores are characterized by low temperature ($T \leq 10$ K) and high density ($n \geq 10^6 \text{ cm}^{-3}$). High depletion of gas phase species has been observed towards prestellar cores (e.g. Tafalla et al. 2004, 2006), suggesting that ice grain mantles are present in these regions. Furthermore ice grain mantles have been observed in quiescent regions of dense molecular clouds (e.g. Chiar et al. 1994, 1995; Whittet et al. 1998; Knez et al. 2005). These results suggest that ice mantles could be as old as the molecular cloud in which they are detected and then suffer from cosmic ion irradiation for a time as long as the molecular cloud's lifetime (e.g. Palumbo & Strazzulla 1993).

Observations have shown that in hot cores and hot corinos the fractional abundance of methyl formate can vary in a wide range of magnitudes, but generally it is on the order of 10^{-7} – 10^{-9} with respect to H₂. The laboratory experiments presented here indicate that after ion irradiation of CO:CH₃OH ice at 16 K the amount of methyl formate is on the order of 10^{-3} with respect to initial methanol. In order to compare our results with the observational data we need to express this value with respect to H₂. In dense molecular clouds the fractional abundance of CO is on the order of 10^{-4} with respect to H₂ (Frerking et al. 1982). Experimental results revealed that CH₃OH can be produced efficiently by successive hydrogenation of CO on grain surfaces at temperatures that are typical in molecular clouds (Watanabe et al. 2007; Fuchs et al. 2009), and the amount of CH₃OH obtained is at least on the order of 10^{-1} with respect

to CO. Other authors suggest that this amount could be higher (Fuchs et al. 2009). Thus if we assume high CO depletion we can say that the fractional abundance of solid CH₃OH is on the order of 10^{-5} with respect to H₂. Moreover, if we assume that methyl formate/methanol column density ratio obtained in the solid state after ion irradiation is maintained in the gas phase after desorption of icy grain mantles, we obtain an amount of methyl formate on the order of 10^{-8} with respect to H₂. This amount is consistent with the observed abundances. For example, the fractional abundance of methyl formate in Sgr B2 N(LMH) is 1.1×10^{-8} (Snyder 2006), in IRAS 16293–2422 B it is $>1.2 \times 10^{-8}$ (Remijan & Hollis 2006), in NGC 2264 MMS it is $(0.7\text{--}5.3) \times 10^{-8}$ (Sakai et al. 2007).

In the light of our results we can propose the model illustrated in Fig. 14. Gas-phase processes produce a high abundance of carbon monoxide, some of which is deposited on the grain surface, where it is partially hydrogenated into formaldehyde and methanol. During their lifetime, icy grain mantles containing CO and CH₃OH interact with low-energy cosmic rays. As a consequence of ion irradiation, methyl formate is produced within interstellar ices. Once this molecule is formed, it can subsequently be released into the gas phase after desorption mechanisms, i.e., when a young stellar object begins to form and the icy mantles sublime.

5. Conclusion

Methyl formate may have played a decisive role in the development of life on our planet. It is therefore crucial to understand what the process of formation of this molecule is in order to include it in the evolutionary models of molecular clouds and to explain the formation of planetary systems. Armed with correct model predictions, it will be possible to conduct meaningful searches of new complex organic molecules. It is likely that different formation processes contribute in different ways at different times of the protostar evolution. We suggested that interaction of icy grain mantles with low-energy cosmic rays could be considered a dominant mechanism in the formation of methyl formate. The analysis of laboratory data allow us to suggest that the gas phase methyl formate observed in the interstellar medium is formed in the solid state after cosmic ion irradiation of icy mantles containing CO and CH₃OH and released to the gas phase after desorption of icy mantles.

Methyl formate has two isomers, glycolaldehyde and acetic acid. Differentiation in the molecular isomers has been observed,

but not explained. Because the set of the three isomers share the same chemical formula ($C_2H_4O_2$), they could also share the same formation process. Our experiments have indeed revealed a weak band that could be attributed to glycolaldehyde. However, we need further and more detailed experimental works to confirm this suggestion. As future work we plan to study the formation of glycolaldehyde and acetic acid after ion irradiation of $CO:CH_3OH$ ice mixtures. Major advances in understanding the formation chemistry of these molecules can come from observational projects like ALMA (Atacama Large Millimeter Array), EVLA (Expanded Very Large Array) and the *Herschel* satellite, all of which expect astrochemistry to be an important component of their scientific programs.

Acknowledgements. The authors wish to thank F. Spinella for his technical assistance in the laboratory, and G. A. Baratta and G. Strazzulla for fruitful discussions during the preparation of this work. This research has been financially supported by the Italian Space Agency contract No. I/015/07/0 (Studi di Esplorazione del Sistema Solare).

References

- Baratta, G. A., & Palumbo, M. E. 1998, *J. Opt. Soc. Am. A*, 15, 3076
- Baratta, G. A., Leto, G., & Palumbo, M. E. 2002, *A&A*, 384, 343
- Bennett, C. J., & Kaiser, R. I. 2007, *ApJ*, 661, 899
- Bennett, C. J., Chen, S. H., Sun, B. J., Chang, A. H. H., & Kaiser, R. I. 2007, *ApJ*, 660, 1588
- Bockelée-Morvan, D., Lis, D. C., Wink, J. E., et al. 2000, *A&A*, 353, 1101
- Boogert, A. C. A., Pontoppidan, K. M., Knez, C., et al. 2008, *ApJ*, 678, 985
- Bottinelli, S., Ceccarelli, C., Lefloch, B., et al. 2004a, *ApJ*, 615, 354
- Bottinelli, S., Ceccarelli, C., Neri, R., et al. 2004b, *ApJ*, 617, 69
- Bottinelli, S., Ceccarelli, C., Williams, J. P., et al. 2007, *ApJ*, 663, 601
- Brown, R. D., Crofts, J. G., Gardner, F. F., et al. 1975, *ApJ*, 197, L29
- Cazaux, S., Tielens, A. G. G. M., Ceccarelli, C., et al. 2003, *ApJ*, 593, 51
- Chiar, J. E., Adamson, A. J., Kerr, T. H., & Whittet, D. C. B. 1994, *ApJ*, 426, 240
- Chiar, J. E., Adamson, A. J., Kerr, T. H., & Whittet, D. C. B. 1995, *ApJ*, 455, 234
- Despois, D., Biver, N., Bockelée-Morvan, D., & Crovisier, J. 2005, in *Astrochemistry: Recent Successes and Current Challenges*, ed. D. C. Lis, G. A. Blake, & E. Herbst (Cambridge University Press), IAU Symp., 231, 469
- Frerking, M. A., Langer, W. D., & Wilson, R. W. 1982, *ApJ*, 262, 590
- Fuchs, G. W., Cuppen, H. M., Ioppolo, S., et al. 2009, *A&A*, 505, 629
- Fulvio, D., Sivaraman, B., Baratta, G. A., et al. 2009, *Spectrochim. Acta A*, 72, 1007
- Gerakines, P. A., Schutte, W. A., & Ehrenfreund, P. 1996, *A&A*, 312, 289
- Gerakines, P. A., Whittet, D. C. B., Ehrenfreund, P., et al. 1999, *ApJ*, 522, 357
- Greenberg, J. M. 1982, in *Comets*, ed. L. L. Wilkening (Tucson: The University of Arizona Press), 131
- Grim, R. J. A., & Greenberg, J. M. 1987, *ApJ*, 321, L91
- Horn, A., Mollendal, H., Sekiguchi, O., et al. 2004, *ApJ*, 611, 605
- Hudson, R. L., & Moore, M. H. 2000, *Icarus*, 145, 661
- Knez, C., Boogert, A. C. A., Pontoppidan, K. M., et al. 2005, *ApJ*, 635, L145
- Kuan, Y. J., Huang, H. C., Charnley, S. B., et al. 2004, *ApJ*, 616, 27
- Ikeda, M., Ohishi, M., Nummelin, A., et al. 2001, *ApJ*, 560, 792
- Maret, S., Ceccarelli, C., Caux, E., Tielens, A. G. G. M., & Castets, A. 2002, *A&A*, 395, 573
- Mennella, V., Baratta, G. A., Esposito, A., Ferini, G., & Pendleton, Y. J. 2003, *ApJ*, 587, 727
- Öberg, K. I., van Dishoeck, E. F., & Linnartz, H. 2009, *A&A*, 504, 891
- Palumbo, M. E., & Strazzulla, G. 1993, *A&A*, 269, 568
- Palumbo, M. E., Castorina, A. C., & Strazzulla, G. 1999, *A&A*, 342, 551
- Palumbo, M. E., Ferini, G., & Baratta, G. A. 2004, *Adv. Sp. Res.*, 33, 49
- Remijan, A. J., & Hollis, H. 2006, *ApJ*, 640, 842
- Remijan, A. J., Friedel, D. N., de Pater, I., et al. 2006, *ApJ*, 643, 567
- Sakai, N., Sakai, T., & Yamamoto, S. 2007, *ApJ*, 660, 363
- Sandford, S. A., & Allamandola, L. J. 1993, *ApJ*, 417, 815
- Sandford, S. A., Aleon, J., Alexander, C. M. O. D., et al. 2006, *Science*, 314, 1720
- Snyder, L. E. 2006, *Proc. Natl. Sci.*, 103, 12243
- Strazzulla, G., & Johnson, R. E. 1991, in *Comets in the post-Halley era*, *ASSL Series*, Dordrecht, 1, 243
- Strazzulla, G., Baratta, G. A., & Palumbo, M. E. 2001, *Spectrochim. Acta Part A*, 57, 825
- Tielens, A. G. G. M., & Hagen, W. 1982, *A&A*, 114, 245
- Watanabe, N., Mouri, O., Nagaoka, T., et al. 2007, *ApJ*, 668, 1001
- Whittet, D. C. B., Gerakines, P. A., Tielens, A. G. G. M., et al. 1998, *ApJ*, 498, L159